Protection Effect of Curcumin for Macrophage-Involved Polyethylene Wear Particle-Induced Inflammatory Osteolysis by Increasing the Cholesterol Efflux

Authors' Contribution:
Study Design A
Data Collection B
Statistical Analysis C
Data Interpretation D
Manuscript Preparation E
Literature Search F
Funds Collection G

ABCDEFG Yu-wei Liu
BCEF Sen-bo An
BC Tao Yang
BC Yue-jun Xiao
BCEF Long Wang
AG Yi-he Hu

Department of Orthopaedics, Xiangya Hospital, Central South University, Changsha, Hunan, P.R. China

Background: Periprosthetic osteolysis, induced by wear particles and inflammation, is a common reason for failure of primary arthroplasty. Curcumin, a nature phenol from plants, has been reported to reduce the inflammation in macrophages. This study aimed to investigate the potential effect of curcumin on macrophage involved, wear particle-induced osteolysis and its mechanism.

Material/Methods: RAW264.7 macrophages were used to test the effects of polyethylene (PE) particles and curcumin on macrophage cholesterol efflux and phenotypic changes. A mouse model of PE particle-induced calvarial osteolysis was established to test the effects of curcumin *in vivo*. After 14 days of treatment, the bone quality of the affected areas was analyzed by micro-computed tomography (micro-CT) and histology, and the bone surrounding soft tissues were analyzed at the cellular and molecular levels.

Results: We found that PE particles can stimulate osteoclastogenesis and produce an M1-like phenotype in macrophages *in vitro*. Curcumin enhanced the cholesterol efflux in macrophages, and maintained the M0-like phenotype under the influence of PE particles *in vitro*. Additionally, the cholesterol transmembrane regulators ABCA1, ABCG1, and CAV1 were enhanced by curcumin *in vivo*. We also found enhanced bone density, reduced osteoclastogenesis, and fewer inflammatory responses in the curcumin treated groups in our mouse osteolysis model.

Conclusions: Our study findings indicated that curcumin can inhibit macrophage involved osteolysis and inflammation via promoting cholesterol efflux. Maintaining the cholesterol efflux might be a potential strategy to prevent periprosthetic osteolysis after total joint arthroplasty surgery.

MeSH Keywords: **Bone Resorption • Cholesterol • Curcumin • Macrophages • Osteolysis**

Full-text PDF: https://www.medscimonit.com/abstract/index/idArt/914197

📄 3469   🖽 1   📊 5   📖 29

Background

Total joint arthroplasty is one of the most successful and cost-effective surgical methods to treat advanced joint diseases [1]. Complications post total joint arthroplasty, such as aseptic loosening and infection, often lead to the implantation failure and severe pain [2]. Prosthesis aseptic loosening and periprosthetic osteolysis, which account for 16.8% of implant failures, are the main reasons for revision total hip arthroplasty [3]. The need for revision total hip arthroplasty is mostly induced by wear particles and particulate debris at the implant-bone interface, which activates macrophage differentiation to osteoclasts, and/or switching phenotype from M0 to inflammatory M1 [4]. Hence, understanding the molecular pathogenesis of periprosthetic osteolysis and how to control macrophage-related inflammation will be of great importance in the design of treatments for periprosthetic osteolysis.

Macrophages can phagocytose the wear particles and particulate debris and produce pro-inflammatory cytokines, such as tumor necrosis factor (TNF-α), interleukin (IL)-6, and IL-1β [4]. These cytokines can activate macrophages to become osteoclasts, which promotes osteoclastogenesis [4–6] and leads to bone resorption and eventually to osteolysis. Researchers have discovered that some small molecules, such as icariin [7], strontium ranelate [8], and dopamine [9], can restrain the wear-particle induced osteolysis and reduce inflammation in animal models, and the *in vivo* evidence suggests potential treatment(s). However, the pharmacological mechanism has not been investigated; thus, side effects of treatments might not be predictable. For example, a risk of venous thrombosis was reported after strontium ranelate treatment [8]. Moreover, this *in vivo* evidence was studied based on metal particles (titanium), which are reported to be the main cause of periprosthetic osteolysis, but titanium implants are less popular in clinically settings these days. Therefore, a better understanding of the polyethylene (PE) based wear particle metabolism may lead to better intervention in the clinic.

Currently, there are many signaling pathways involved in wear particle induced periprosthetic osteolysis. For example, PE-wear particles can induce toll-like receptor (TLR) signals to initiate nuclear factor κB (NFκB) activation, leading to the secretion of inflammatory cytokines in macrophages, dendritic cells and other monocytic lineages [10]. Interestingly, the cholesterol accumulates in macrophages, triggering pro-inflammatory signals and amplifying the TLR pathway, which has always been related to the inflammatory response such as in atherosclerosis [11]. To maintain the systematic homeostasis, the human body has its own counter-regulatory mechanism to cholesterol accumulation in macrophages – the process of reverse cholesterol transport [12]. Inflammatory lipids in macrophages that are phagocytosed from peripheral tissue are transported into the

circulation and returned to the liver and gallbladder, thus maintaining the systematic homeostasis. Cholesterol efflux is the first step of reverse cholesterol transport at the cellular level, regulated by the transmembrane transporters such as ATP-binding cassette (ABC) transporters ABCA1 and ABCG1 [13]. Cholesterols are carried by caveolin-1 (CAV-1), which transports cholesterols from intracellular compartments into caveolae, and to high-density lipoproteins (HDLs) via the transmembrane transporters into the circulation and eventually to the liver [14].

Curcumin is an active natural phenol compound that can be extracted from the perennial *Curcuma longa,* and serves as an herbal medicine for many disease [15]. Curcumin has multiple functions, including as anti-inflammatory, antihepatotoxic, and antihyperlipidemic [15], which share similar transmembrane transport biological processes in different cell types. A previous study showed that curcumin increases the ABCA1-mediated cholesterol efflux and inhibits macrophage-related inflammation and apoptosis in atherosclerosis [16].

It has also been reported that curcumin can inhibit the NF-κB in osteoclast precursors [17]. Therefore, we hypothesized that curcumin might prevent PE particle induced inflammatory osteolysis by enhancing cholesterol efflux in macrophages. In this study, we used the RAW 264.7 macrophage cell line model with PE particle and curcumin treatment in a mouse model of PE particle-induced calvarial osteolysis to test the potential functions and mechanism of curcumin both *in vitro* and *in vivo*.

Material and Methods

Cell culture

Mouse monocyte/macrophage Raw264.7 cells (Chinese Academy of Science, Shanghai, China) ($1×10^6$ cells/well) were cultured into 6-well plates in RPMI 1640 medium supplemented with 10% fetal calf serum (FBS) (complete medium; Gibco, Thermo Fisher Scientific, Waltham, MA, USA) at 37°C in a 5% CO_2 incubator. The cells were cultured in medium alone (blank group) or were treated in triplicate with 1 mg/mL of PE (PE group), 1 mg/mL of PE plus 10 μM curcumin (Sigma Aldrich), or 1 mg/mL of PE plus 20 μM curcumin for 72 hours, respectively. The PE were added to and suspended in culture medium. Curcumin was treated at 0.5 hours post PE treatment. For osteoclast formation, 50 ng/mL of RANKL (Sigma Aldrich, USA) was added to the medium.

Cholesterol efflux test

RAW264.7 cells ($1×10^4$ cells/well) were cultured in 96-well plates in complete medium for 2 hours and were treated in duplicate with different concentrations (0, 1, 5, 10, 20 μM) of

curcumin for 2 days. The cells were incubated with 1 µCi/mL of [³H] cholesterol (Perkin Elmer, Boston, USA) in serum-free medium (RPMI 1640 medium containing 0.2% fatty acid-free bovine serum albumin) at 37°C for 24 hours. After the cells were equilibrated in the serum-free medium for 18 hours, they were incubated with 50 µg/mL HDL (Yiyuan Biotech, Guangzhou, China) in serum-free medium for 4 hours to induce the cholesterol efflux. The culture media and cell lysate were then collected. Cholesterol efflux was calculated as the ratio (%) of the radiotracer in the medium to the total (medium + cells).

Animal model for PE particle-induced calvarial osteolysis

Male BALB/C mice were acquired from the Experimental Animal Center, Central South University. All the mice were housed in a specific pathogen-free facility with a controlled constant temperature (20±0.5°C), a 12-hour: 12-hour light/dark cycle, and free access to water and food. All experimental protocols were performed according to the Ethical Guidelines of the International Association for the Study of Pain [18] and were approved by the Animal Care and Use Committee of Central South University (NO. 201512542).

A mouse model of PE particle-induced calvarial osteolysis was established, as described previously [19]. Briefly, individual BALB/C mice were anaesthetized, and the skull was subjected to a 10-mm midline incision over the calvarium to expose approximately 0.25 cm^2 of the calvarium. The control mice received no particles (blank group), and the incision was closed without any further intervention. The remaining mice received 10 mg of dried PE particles (40–48 µm in diameter; Sigma Aldrich, USA) that had been sterilized with 70% ethanol for 24 hours, followed by incision closure. The PE-treated mice were randomized and treated intraperitoneally with solvent (5% DMSO and 95% corn oil) or curcumin (Sigma Aldrich) in solvent daily for 14 consecutive days, respectively. There were 4 groups, including the blank group (sham surgery and solvent), the PE-particle group (PE and solvent), the low Cur group receiving 0.5 µM curcumin in 25 µL of solvent per injection (10 mg/kg body weight), and the high Cur group receiving 1 µM curcumin treatment in 25 µL solvent per injection (20 mg/kg body weight) (n=5 for each group). At the end of the experiment, all mice were sacrificed, and their calvarias and bone surrounding soft tissue were dissected for micro-computed tomography (micro-CT) and histological examinations, western blot analysis, and qPCR. The tissues in the ROIs (regions of interesting) were used for immunohistochemical analysis and TRAP (tartrate-resistant acid phosphatase) staining.

Micro-CT

The calvarial specimens were evaluated using micro-CT, as described previously [20,21]. The calvaria was cautiously dissected from individual mice, fixed, and scanned using a micro-CT scanner (µCT100; SCANCO Medical AG, Brüttisellen, Switzerland). The reference lines were created by a holder in 20 µm voxels (volume elements) reconstruction to define the analysis area. The operation of microfocus x-ray tube was 70 Kv, 200 µA, 360° rotation under 300 ms exposure per view. The mineral density of the skull cavity of the calvarial samples were evaluated for the tissue volume (TV; mm^3), bone volume (BV; mm^3), relative volume of calcified tissue in the selected volume of interest VOI (BV/TV) and trabecular thickness (Tb.Th, µm) using a 3D analysis software of SCANCO Medical.

TRAP staining

The mouse skull flaps were fixed with 4% paraformaldehyde for 24 hours, and decalcified every 2 days in fresh EDTA decalcifying solution (gifted by Pathology Department, Xiangya Hospital) for 30 to 40 days. The flaps were paraffin-embedded and the flap tissue section (4 µm) was stained with TRAP using the TRAP kit (Sigma-Aldrich), according to the manufacturer's instructions. The images were captured under a light microscope (Leica DM 2500, Leica Microsystems GmbH, Germany). The TRAP-positive cell number was measured using TRAP-positive multinucleated cells with more than 3 nuclei counted from 6 randomly-selected visual fields.

Western blot analysis

The collected Raw264.7 cells and bone surrounding soft tissues were homogenized and lysed in lysis buffer including RIPA and phenylmethanesulfonyl fluoride (PMSF; Beyotime Institute of Biotechnology, Haimen, Jiangsu, China). The lysates (30 µg/lane) were separated on 10% gels and were transferred onto polyvinylidene difluoride membranes (Beyotime Institute of Biotechnology). The membranes were blocked with 5% (w/v) BSA in Tris-buffered saline with 0.1% (w/v) Tween 20 (TBST) and probed with primary antibodies: mouse anti-ABCA1 (1: 1000; Abcam Biotechnology), rabbit anti-ABCG1 (1: 2500; Abcam Biotechnology), rabbit anti-Cav-1 (1: 1500; Abcam Biotechnology), rabbit anti-TNF-α (1: 1000; Abcam Biotechnology), rabbit anti-IL-6 (1: 1000; Cell Signaling Technology), rabbit anti-IL-1β (1: 1,000; Abcam Biotechnology), and mouse anti-β-actin (1: 4000; Proteintech, Rosemont, USA) at 4°C overnight. After washing, the bound antibodies were detected using optimal horseradish peroxidase-conjugated secondary antibodies: goat anti-rabbit IgG (1: 10 000) and goat anti-mouse IgG (1: 10 000; Merck Millipore, Darmstadt, Germany) and were visualized using the enhanced chemiluminescence reagents (Bio-Rad Laboratories, Hercules, USA). The relative levels of the target proteins to that of control β-actin were analyzed densitometrically using the Quantity One software (version 4.0, Bio-Rad).

Table 1. The sequences of primers.

Gene primers	Sequences
ABCA1	Forward 5'-AAGGGGTGGTGTTCTTCCTC-3' and reverse 5'-CCTCACATCCTCATCCTCGT-3' (113 bp)
ABCG1	Forward 5'- CTTTGATGAGCCCACCAG-3' and reverse 5'-CGCATTGTCCTTGACTTAG-3' (170 bp)
CAV1	Forward 5'-TCAAGATTGACTTTGAAGATGTG-3' and reverse 5'-GGAGAGAATGGCAAAGTAAATG-3' (179 bp)
TNF-α	Forward 5'-CACTCACAAACCACCAAG-3' and reverse 5'-GGTTGTCTTTGAGATCC-3' (93 bp)
IL-6	Forward 5'-AGAAAAGAGTTGTGCAATG-3' and reverse 5'-CCAGAAGACCAGAGGAAA-3' (160 bp)
IL-1β	Forward 5'-CACCTTTTGACAGTGATGA-3' and reverse 5'-CAGCCACAATGAGTGATAC-3' (174 bp)
GAPDH	Forward 5'-GGTGAAGGTCGGTGTGAACG-3' and reverse 5'-CTCGCTCCTGGAAGATGGTG-3' (233 bp)

Real-time quantitative PCR

Total RNA was extracted from Raw 264.7 cells and the repaired tissues using TRIZol (Invitrogen, Thermo Fisher Scientific, USA) according to the manufacturer's instructions. The RNA samples (1 µg/each) were reverse transcribed into cDNA using the First Strand cDNA Synthesis Kit (GeneCopoeia, USA) following the manufacturer's instructions. The relative levels of the target gene mRNA transcripts in individual samples were determined by quantitative PCR using the Applied Biosystems 7700 Real-time PCR system (Thermo Fisher Scientific, Inc., USA), the SYBR Green Real-time PCR Master Mix (TOYOBO, Japan) and specific primers. The sequences of primers are listed in Table 1. The PCR reactions were performed in duplicate at 95°C for 2 minutes and were subjected to 45 cycles of 95°C for 15 seconds, 58°C for 15 seconds, and 72°C for 45 seconds. The data were normalized to *Gapdh* and were calculated by the $2^{-\Delta\Delta Ct}$ method.

Statistical analysis

The data are means ± standard deviations (SDs). The difference among groups was analyzed by one-way ANOVA using GraphPad Prism software, version 5.0 (GraphPad Software, CA, USA). A *P* value <0.05 was considered statistically significant.

Results

Curcumin reduces PE-particle induced osteoclastogenesis

To analyze the effect of curcumin on osteoclastogenesis, we cultured the RAW264.7 cells in growth medium containing RANKL (50 ng/mL). We have found that PE particles in culture medium could stimulate macrophages activation and maturation (Figure 1). The average diameter of RAW264.7 cells was significantly increased in the PE treated groups, indicating a matured macrophage morphology (Figure 1A, 1B). The activated osteoclast marker TRAP was also stimulated by PE in macrophages (Figure 1A, 1C). Adding curcumin into the culture medium could significantly reduce the TRAP$^+$ cell numbers, and it tended to follow a dose-dependent manner (Figure 1C).

Curcumin inhibits PE-induced macrophage polarization via enhanced cholesterol efflux
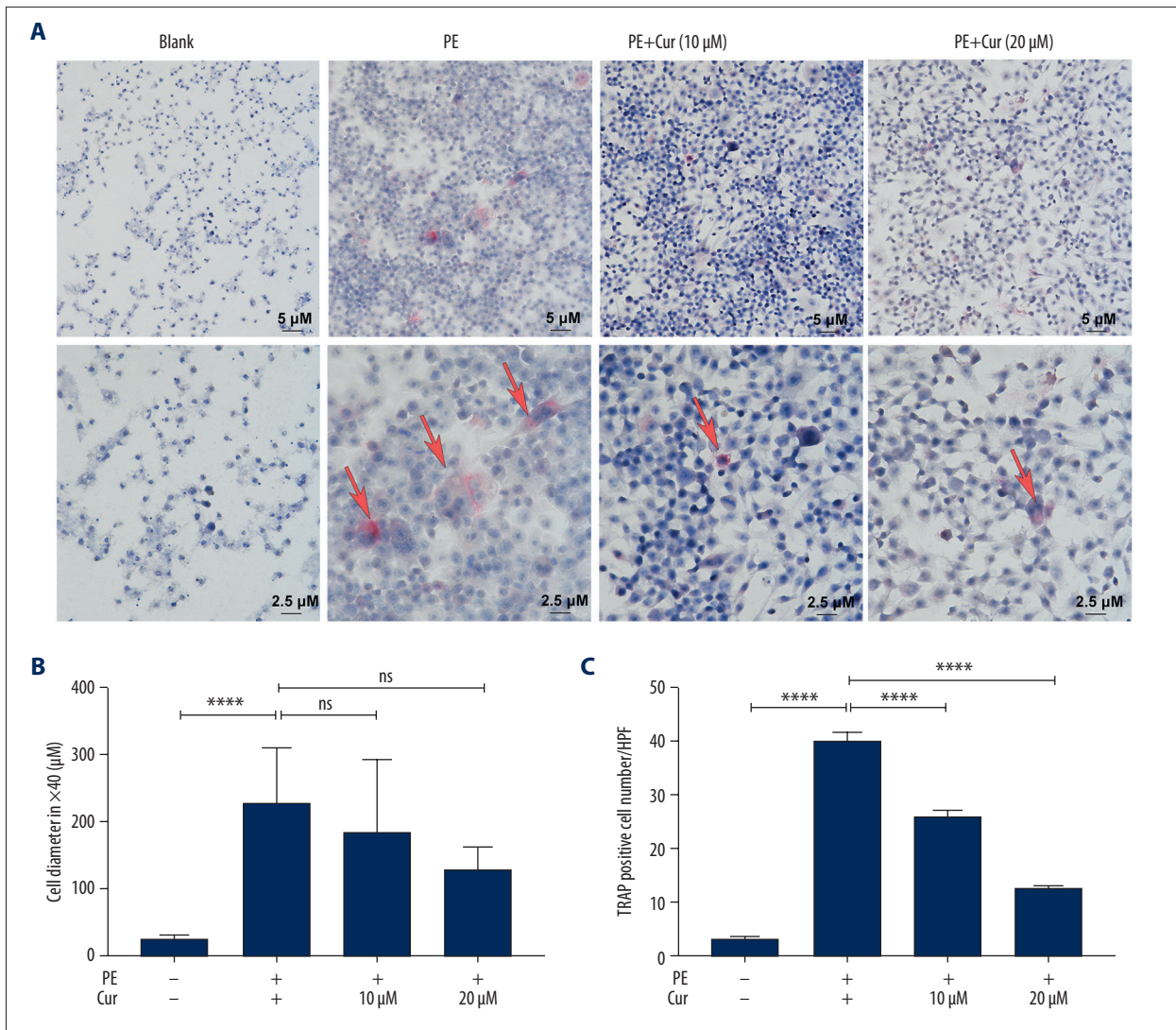
We further analyzed the effects of curcumin treatment on the macrophage polarization. The pro-inflammatory cytokine production of TNF-α, IL-1β, and IL-6 was significantly increased by PE particles, indicating an M1-like macrophage phenotypic polarization [22] (Figure 2A). Curcumin treatment significantly reduced the protein expression levels of TNF-α, IL-1β, and IL-6, as compared with those in the PE particle-treated cells (Figure 2A).

To investigate whether the curcumin had functioned by affecting cholesterol metabolism in macrophages (Figure 2B), we evaluated the cholesterol efflux in macrophages using the [^{3}H] cholesterol labelling assay. We found that treatment with curcumin significantly increased the percentages of free cholesterol in the supernatants of cultured macrophages in 10 µM group (Figure 2C). In addition, western blotting also revealed that treatment with curcumin significantly increased the protein expression levels of cholesterol transporter proteins ABCA1 and ABCG1 and cholesterol carrier protein CAV1, as compared with that in the PE particle-treated cells (Figure 2D), indicating the cells were in an activated cholesterol transportation state.

Collectively, treatment with curcumin significantly mitigated PE particle-induced osteoclastogenesis and macrophage polarization, which could be due to enhanced cholesterol efflux.

Curcumin prevents PE particles induced calvarial osteolysis *in vivo*

To further study the effect of curcumin *in vivo*, a mouse model of calvarial osteolysis was established by open surgery and directly spreading PE particles over the calvarium (PE group). The mice were injected with 25 µL of solvent or curcumin in

This work is licensed under Creative Common Attribution-NonCommercial-NoDerivatives 4.0 International (CC BY-NC-ND 4.0)

13

Indexed in: [Current Contents/Clinical Medicine]   [SCI Expanded]   [ISI Alerting System]
[ISI Journals Master List]   [Index Medicus/MEDLINE]   [EMBASE/Excerpta Medica]
[Chemical Abstracts/CAS]

Figure 1. Curcumin inhibits PE-particle-induced osteoclastogenesis *in vitro*. Osteoclastogenesis in RAW264.7 cells were induced with PE particles (1 mg/mL), and the effects of curcumin were tested at different concentrations (10 µM, 20 µM). Cells were cultured in growth medium with 50 ng/mL RANKL (blank group), were treated with PE (PE group) and curcumin (PE+Cur) for 3 days, and were stained with tartrate-resistant acid phosphatase (TRAP, red stain) (**A**). The average diameter of RAW264.7 cells at 40× magnification which was measured using ImageJ software (**B**). TRAP staining and quantitative analysis of TRAP+ cells and TRAP+ cell number in high magnification per field (**C**). The data are representative images or are expressed as the means ±SD of each group from 3 separate experiments with 3 technical repeats in each experiment. * $P<0.05$, ** $P<0.01$, *** $P<0.001$, and **** $P<0.0001$. PE – polyethylene; Cur – curcumin; TRAP – tartrate-resistant acid phosphatase; SD – standard deviation.

solvent (0.5 µM in 25 µL (10 mg/kg), 1 µM in 25 µL (20 mg/kg)) daily for 14 days to determine the potential therapeutic effect.

The calvaria of each mouse was examined using micro-CT images (Figure 3A). A wide range of bone resorption in the calvaria was found in the PE-particle exposure group, but not in the blank group, and quantitative analysis showed significantly decreased bone mineral density (BMD) levels and reduced ratios of BV/TV and Tb.Th, a hallmark of the calvarial osteolysis, in the PE group, as compared with that in the blank group, indicating a successful calvarial osteolysis model.

There were obvious surface erosions centered at the midline of the parietal bones in the PE group, and fewer erosions in the curcumin treated groups with increasing concentrations. Additionally, the range of bone resorption was significantly less in the 1 µM/day group than that in the 0.5 µM/day group of the curcumin treatment groups. The quantitative analysis data showed no significant differences between the 1 µM daily curcumin treatment group and blank group in terms of BMD, the BV/TF ratio, and Tb.Th, indicating that the administration of curcumin at a level of 1 µM daily treatment could prevent the development of PE-induced calvarial osteolysis.
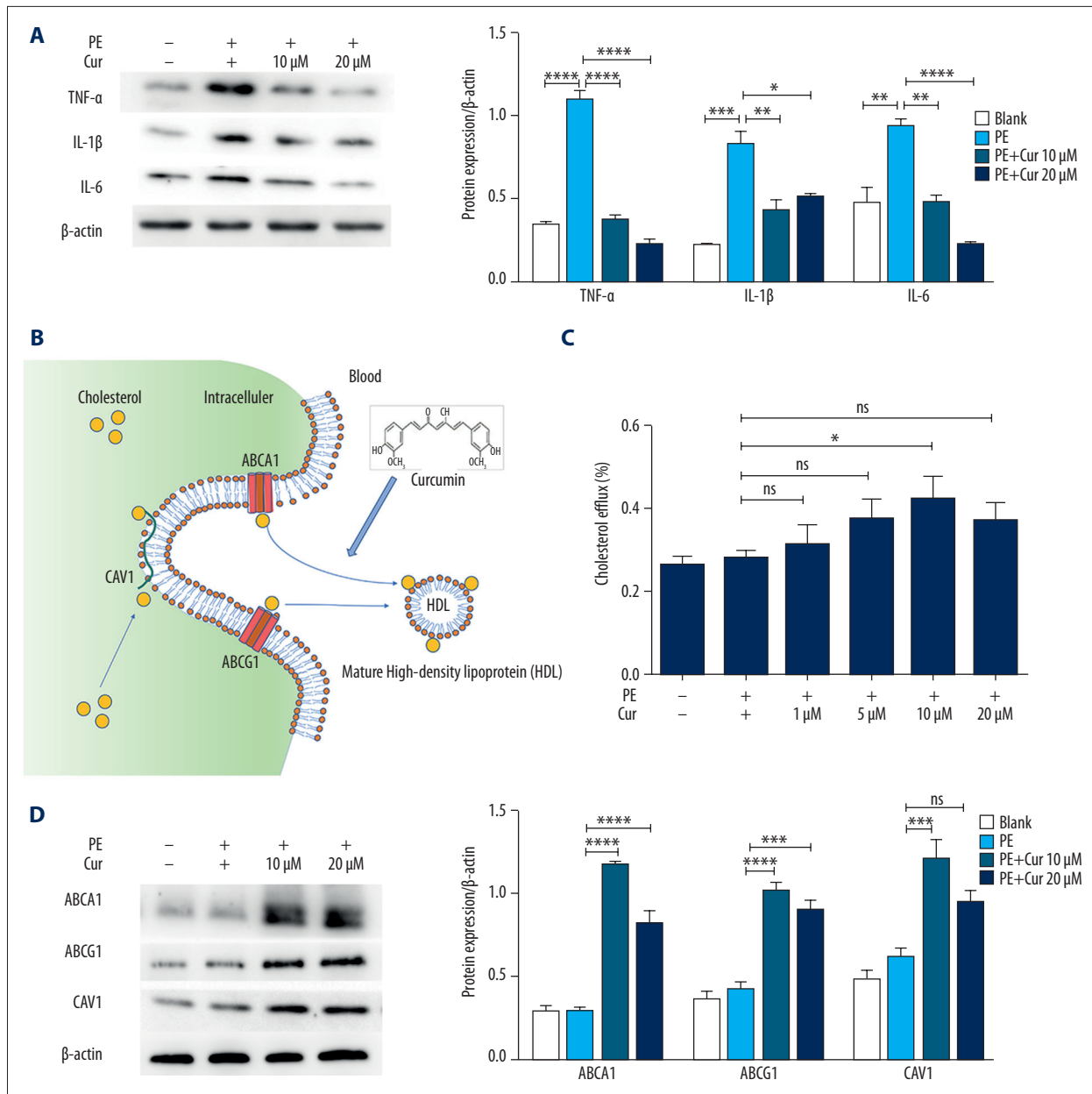
Figure 2. Curcumin inhibits PE-induced M1 polarization of macrophage via enhanced cholesterol efflux. The effects of curcumin on cholesterol efflux (**A–D**) and macrophage polarization were further tested in PE-induced RAW264.7 cells *in vitro*. Cells were cultured in basal medium (blank group) and were treated with PE particles (1 mg/mL, PE group) and curcumin at different concentrations (1, 5, 10, 20 μM PE+Cur group). Proposed function of curcumin in cholesterol metabolism (**A**). Curcumin enhances cholesterol efflux in macrophages. CAV1, Caveolin 1, cholesterol carrier protein; ABCA1, ATP-binding cassette transporter, sub family A1, also known as cholesterol efflux regulatory protein; ABCG1, ATP-binding cassette sub-family G member 1, cholesterol transporter protein. Cholesterol efflux analysis (**B**). Cells were treated with PE and curcumin for 48 hours and then were subjected to ^{3}H-choletserol analysis. The ratio (%) of ^{3}H-labelled free cholesterol in the supernatant versus the total ^{3}H-labled cholesterol in both supernatant and cell was defined as the cholesterol efflux. The expression levels of cholesterol transporters ABCA1, ABCG1 and cholesterol carrier CAV1 in macrophages (**C**). Western blot and quantitative analyses of ABCA1, ABCG1, and CAV1. β-actin was used as the loading control (**C**). Curcumin inhibits PE-induced macrophage polarization (**D**). Western blot and quantitative analyses of the protein expression levels of TNF-α, IL-1β, and IL-6, the M1 macrophage markers. β-actin was used as loading control (**D**). The data are representative images or are expressed as the means ±SD of each group from 3 separate experiments with at least duplicates. * $P < 0.05$, ** $P < 0.01$, and *** $P < 0.001$. PE – polyethylene; Cur – curcumin; TNF – tumor necrosis factor; IL – interleukin; SD – standard deviation.

15

Indexed in: [Current Contents/Clinical Medicine]   [SCI Expanded]   [ISI Alerting System]
[ISI Journals Master List]   [Index Medicus/MEDLINE]   [EMBASE/Excerpta Medica]
[Chemical Abstracts/CAS]

Histological examinations of the ROIs revealed that there were many inflammatory infiltrates in the calvarias of PE particle-treated mice (Figure 3B). A similar pattern of TRAP staining was detected in the different groups of mice, and quantitative analysis indicated that treatment with curcumin significantly minimized the numbers of TRAP-positive cells in the calvarias of mice (Figure 3C, 3D). Collectively, these data indicated that treatment with curcumin significantly inhibited the PE particle-induced calvarial osteolysis in mice.
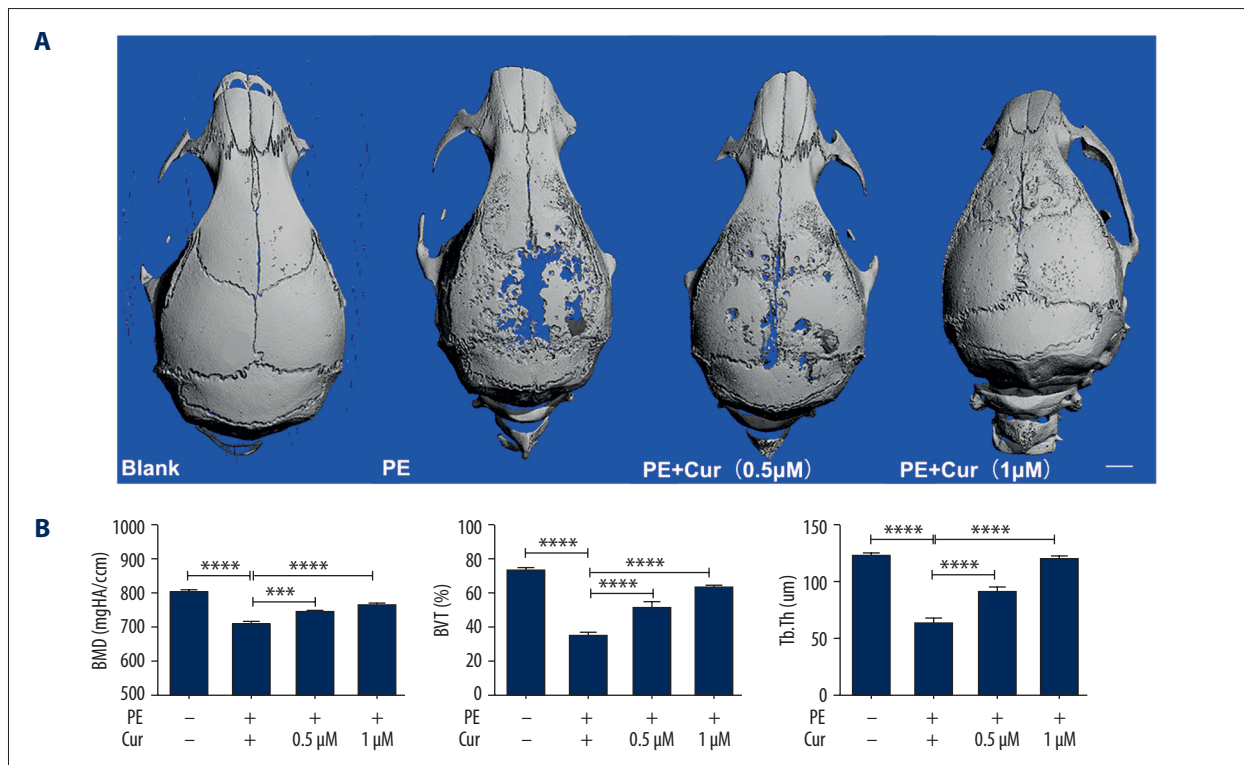
Curcumin attenuates inflammatory responses and enhances the cholesterol efflux in PE particle affected soft tissue
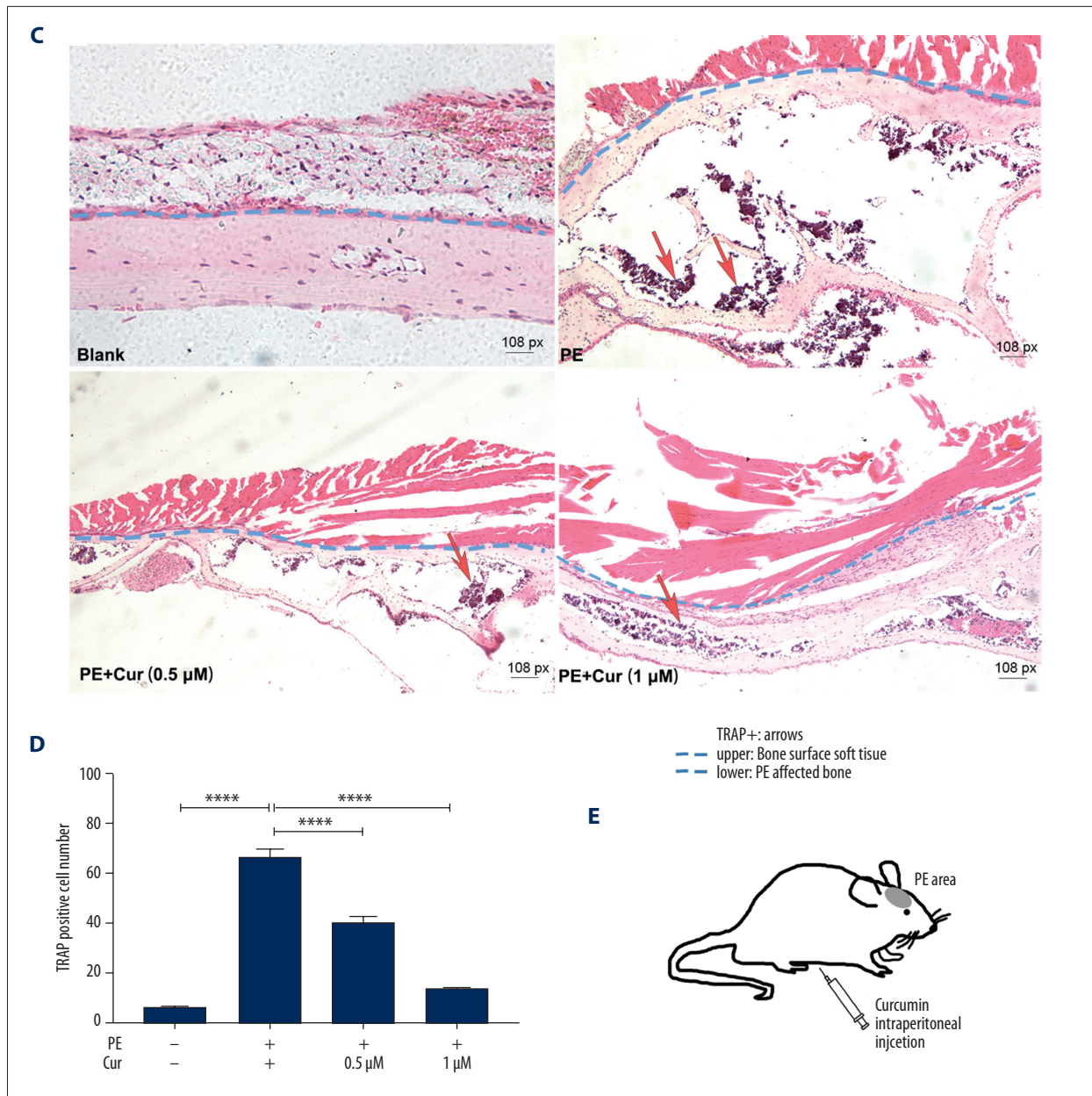
To examine the effect of curcumin on soft tissues of the ROIs, we isolated the periosteum and subcutaneous tissue of the PE particle affected area and investigated the expression of key pro-inflammatory cytokines TNF-α, IL-6, and IL-1β at both the protein and mRNA levels. Significantly elevated levels of TNF-α, IL-6, and IL-1β were detected in the eroded bone surface soft tissues after implantation with PE particles (Figure 4A). By contrast, the quantity of these cytokines was reduced in the curcumin treated groups with the increase in concentration. A similar pattern of the relative mRNA expression levels of *TNF-α*, *IL-6*, and *IL-1β* was also detected (Figure 4C). Thus, curcumin treatment significantly mitigated inflammatory responses in the soft tissue of PE particle induced calvarial osteolysis mice.

To evaluate whether curcumin functioned by enhancing the cholesterol efflux *in vivo*, the levels of the transmembrane transporters and carrier of cholesterol, ABCA1, ABCG1 and CAV1, were determined by western blotting and qPCR. Although the PE particles did not alter the ABCA1, ABCG1, and CAV1 protein expression levels in the bone surface soft tissues of the ROIs (Figure 4B), curcumin treatments significantly increased the relative levels of ABCA1, ABCG,1 and CAV1 with the increase in concentration (Figure 4B). A similar pattern of the relative mRNA expression levels of *Aabc1*, *Abcg1*, and *Cav1* was detected (Figure 4C). The enhanced ABCA1, ABCG1, and CAV1 expression levels in tissues by curcumin suggested that curcumin treatment might function by enhancing cholesterol efflux in the bone surface soft tissue to prevent calvarial osteolysis.

Discussion

Wear particles from joint prostheses could trigger the granulomatous chronic inflammation in the periprosthetic tissue that interrupts bone metabolism and eventually leads to periprosthetic osteolysis [3]. Monocytes/myeloid blasts from blood or bone marrow are recruited to the periprosthetic tissue and differentiate into resident macrophages and osteoclasts under the influence of wear particles [10,23]. In this study, we have found that curcumin could prevent the development of PE particle induced periprosthetic osteolysis via promoting cholesterol efflux in macrophages.

This work is licensed under Creative Common Attribution-NonCommercial-NoDerivatives 4.0 International (CC BY-NC-ND 4.0)

16

Indexed in: [Current Contents/Clinical Medicine] [SCI Expanded] [ISI Alerting System] [ISI Journals Master List] [Index Medicus/MEDLINE] [EMBASE/Excerpta Medica] [Chemical Abstracts/CAS]

Figure 3. Curcumin prevents PE particle-induced calvarial osteolysis in mice. BALB/c mice were induced to undergo calvarial osteolysis by embedding PE particles (10 mg) between the calvarial bone and soft tissue. The mice were randomized and treated with curcumin (0.5 µM and 1 µM, daily) intraperitoneally for 14 days. The control group received both sham surgery and the solvent of curcumin (5 animals per group). The BMD, BV/TV and Tb.Th in the calvaria in individual mice were evaluated by micro-CT (**A, B**). The calvarial tissues were stained using TRAP (blue dotted line separating bone surface soft tissue (upper) and PE affected bone (lower)) (**C, D**), respectively. The data are representative images or are expressed as the mean ±SD (n=5). * $P<0.05$, ** $P<0.01$, ***, **** $P<0.001$, and ***** $P<0.0001$. A diagram for the mouse model of PE-induced calvarial osteolysis (**E**). PE – polyethylene; micro-CT – micro computed tomography; TRAP – tartrate-resistant acid phosphatase; SD – standard deviation.

Curcumin has been demonstrated to have the anti-inflammation activity in chronic diseases [24]. This highly pleiotropic molecule was also reported to have antioxidant, antibacterial, anti-fungal, anti-viral, anti-inflammatory, anti-proliferative, and pro-apoptotic effects [24]. It is questionable how a single agent could exhibit all these effects. Interestingly, it was reported that curcumin could affect cholesterol metabolism by enhancing the cholesterol efflux in macrophages [25] and adipocytes [26], possibly explaining the multiple effects of curcumin. By regulating the cholesterol metabolism, curcumin
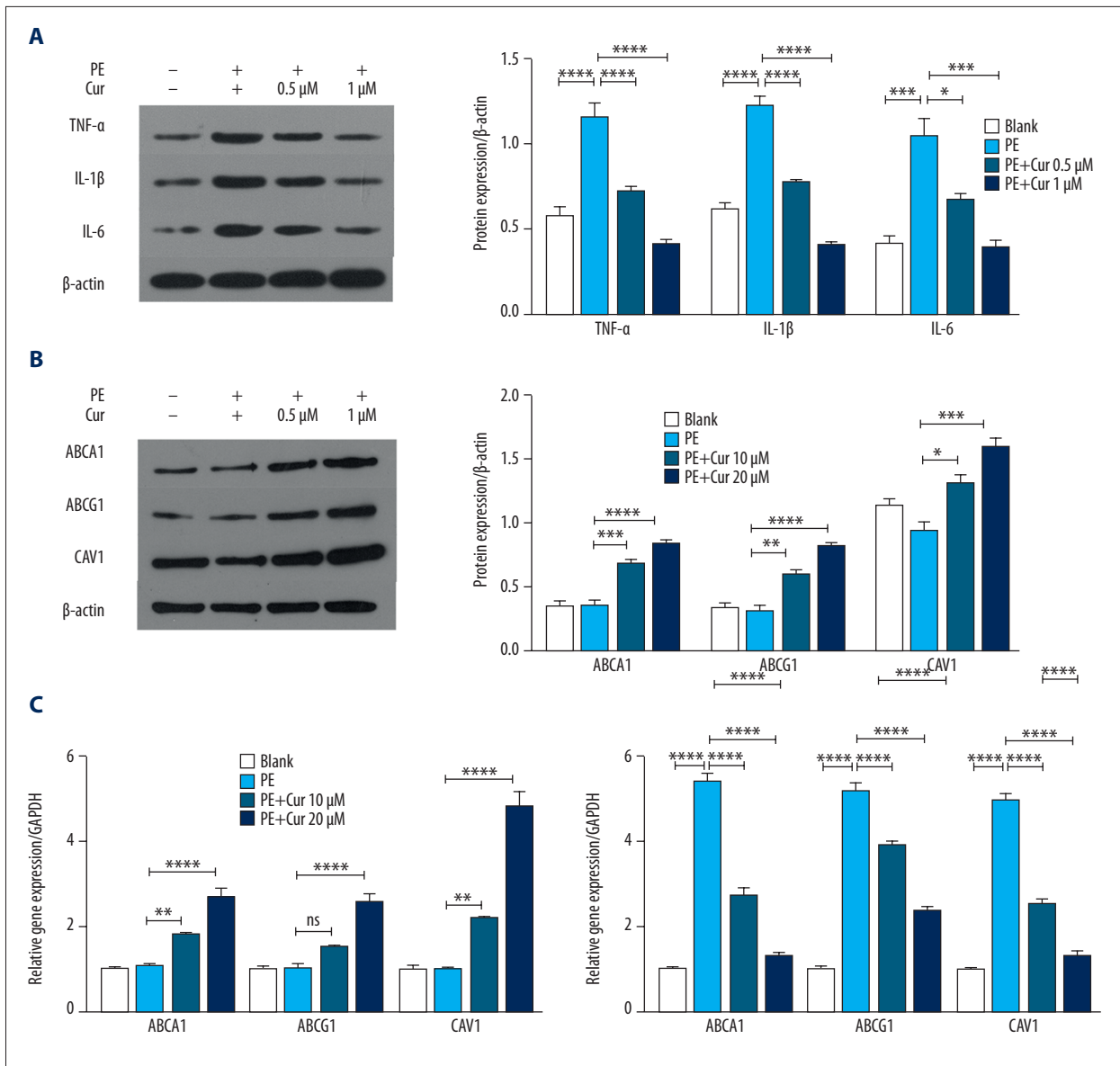
Figure 4. Cellular and molecular signatures of bone surface soft tissues in curcumin preserved calvarial osteolysis. The relative protein and mRNA expression levels of *Tnf-α, IL-6, IL-1*β*, Abca1, Abcg1* and *Cav1* in the bone surface soft tissue of the ROIs (n=5) were determined by western blotting and qPCR. The data are representative images or are expressed as the means ±SE of one batch representative experiment with triplicates from 3 separate experiments. (**A**) Western blot and quantitative analyses of TNF-α, IL-6, and IL-1β. (**B**) Western blot and quantitative analyses of ABCA1, ABCG1, and CAV1. β-actin was used as the loading control. (**C**) Quantitative PCR analysis of the mRNA expression levels of *Tnf-α, Il-6, Il-1*β*, Abca1, Abcg1, Cav1* and housekeeping gene, *Gapdh*. * *P*<0.05, ** *P*<0.01, *** *P*<0.001, and **** *P*<0.0001. TNF – tumor necrosis factor; IL – interleukin; CAV1 – caveolin-1; ROI – region of interest.

could directly affect cell signaling transduction, which is a very basic biological process in all living cells.

In our study, we found that PE particles could induce macrophage polarization (enhanced TNF-α, IL-1β, and IL-6 production), and enhance the osteoclastogenesis (TRAP+, multinucleated giant cells formation) in RAW264.7 cell cultures

in vitro, and curcumin significantly attenuated these effects that are induced by PE particles. More importantly, we also found that curcumin treatment significantly enhanced cholesterol efflux and upregulated cholesterol carriers and transporters such as CAV1, ABCA1, and ABCG1 expression in macrophages. Therefore, enhancing the cholesterol efflux in macrophages could be a potential strategy to prevent and
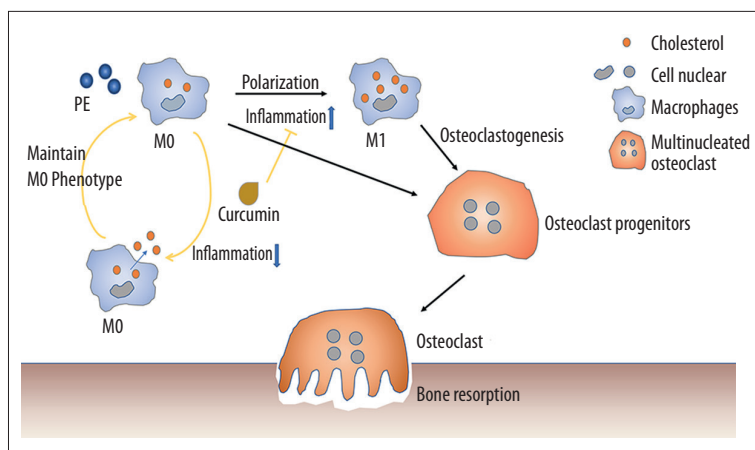
Figure 5. Proposed mechanism of the intercellular cholesterol levels in macrophage phenotypic changes and differentiation. PE particle-stimulated macrophage phenotypic changes (M0 to M1) can be inhibited by curcumin treatment, thus reducing further osteoclastogenesis and bone loss. M0 – non-polarized macrophage; M1 – M1-macrophage; PE – polyethylene.

inhibit the development of wear particle induced periprosthetic osteolysis.

We further used a mouse model to confirm our hypothesis *in vivo* and found that treatment with curcumin could significantly mitigate PE particle induced calvarial osteolysis by minimizing or preventing calvarial bone damages. A wide range of bone resorption in the calvaria was found with the PE particle exposure group at day 14, and no differences were found between the blank and 1 μM curcumin treatment group in the bone mineral density (BMD) level, BV/TV, and Tb.Th, but the bone surrounding soft tissue was clearly thickened in the PE+Cur group compared with that in the no PE group. From the analysis at molecular level of the bone surrounding soft tissue, we confirmed upregulated ABCA1, ABCG1, and CAV-1 expression in the calvarial surround soft tissues and reduced expression of TNF-α, IL-1β, and IL-6 in the curcumin treated group compare with that in the PE particle group. These molecular signatures indicated an actively cholesterol metabolism status in the soft tissue surrounding bone, which could be the reason for the bone protection effect in the PE particle induced osteolysis.

Based on our *in vitro* and *in vivo* results, we propose a possible mechanism for the function of curcumin on the prevention of osteolysis (Figure 5). M0 macrophages can be stimulated by PE particles and turn into the M1 phenotype, which is a regular PE particle induced inflammatory response, and then the M1 macrophages would differentiate into pre-osteoclasts, with the stimulation of inflammatory factors eventually to become mature osteoclasts to induce bone loss. Curcumin treatment inhibiting the bone loss in periprosthetic osteolysis could be due to curcumin enhancing the macrophage cholesterol efflux, thus maintaining the macrophage M0 phenotype.

Despite the positive *in vitro* results, the poor absorption of curcumin by oral administration has been a major problem for its clinical application [27]. Recent studies have pointed out that curcumin is an unstable, reactive, and nonbioavailable compound [28]. To overcome this problem, we used an oil-based solvent (5% DMSO and 95% corn oil) to dissolve curcumin and deliver the drug daily at a relative low concentration (0.5–1 μM), and we showed a successful bone protection effect from PE-induced calvarial osteolysis.

One limitation of this study was that the murine calvarial bone is a flat bone model, which may not completely reflect the long bone situation in the human body – the mechanical load, fluid pressure, and continuous generation of wear particles are all more complicated. Moreover, this osteolysis model was performed for 2 weeks, and a longer effect and higher dosage of curcumin in larger animals should be investigated in the future. In addition, osteolysis is the result of the failure of local tissue homeostasis by which many types of cells, such as osteoclasts and osteoblasts, are involved [29]. Therefore, it is also important to determine the role of curcumin in regulating the osteoblasts in the future.

Conclusions

We found that curcumin could prevent PE particle-induced calvarial inflammatory osteolysis via enhancing cholesterol efflux in macrophages. Our findings may provide new insights into the pharmacological action of curcumin in inhibiting PE particle-induced osteolysis.

Acknowledgements

References:

1. Pivec R, Johnson AJ, Mears SC, Mont MA: Hip arthroplasty. Lancet, 2012; 380: 1768–77

2. Vanhegan IS, Malik AK, Jayakumar P et al: A financial analysis of revision hip arthroplasty: the economic burden in relation to the national tariff. J Bone Joint Surg Br, 2012; 94: 619–23

3. Cobelli N, Scharf B, Crisi GM et al: Mediators of the inflammatory response to joint replacement devices. Nat Rev Rheumatol, 2011; 7: 600–8

4. Nich C, Takakubo Y, Pajarinen J et al: Macrophages-key cells in the response to wear debris from joint replacements. J Biomed Mater Res A, 2013; 101: 3033–45

5. Wang CT, Lin YT, Chiang BL et al: Over-expression of receptor activator of nuclear factor-kappa B ligand (RANKl), inflammatory cytokines, and chemokines in periprosthetic osteolysis of loosened total hip arthroplasty. Biomaterials, 2010; 31: 77–82

6. Chiu R, Ma T, Smith RL, Goodman SB: Ultrahigh molecular weight polyethylene wear debris inhibits osteoprogenitor proliferation and differentiation *in vitro*. J Biomed Mater Res A, 2009; 89: 242–47

7. Shao H, Shen J, Wang M et al: Icariin protects against titanium particle-induced osteolysis and inflammatory response in a mouse calvarial model. Biomaterials, 2015; 60: 92–99

8. Liu X, Zhu S, Cui J et al: Strontium ranelate inhibits titanium-particle-induced osteolysis by restraining inflammatory osteoclastogenesis *in vivo*. Acta Biomater, 2014; 10: 4912–18

9. Yang H, Xu Y, Zhu M et al: Inhibition of titanium-particle-induced inflammatory osteolysis after local administration of dopamine and suppression of osteoclastogenesis via D2-like receptor signaling pathway. Biomaterials, 2016; 80: 1–10

10. Kandahari AM, Yang X, Laroche KA et al: A review of UHMWPE wear-induced osteolysis: The role for early detection of the immune response. Bone Res, 2016; 4: 16014

11. Tall AR, Yvan-Charvet L: Cholesterol, inflammation and innate immunity. Nat Rev Immunol, 2015; 15: 104–16

12. Rader DJ, Tall AR: The not-so-simple HDL story: Is it time to revise the HDL cholesterol hypothesis? Nat Med, 2012; 18: 1344–46

13. Phillips MC: Molecular mechanisms of cellular cholesterol efflux. J Biol Chem, 2014; 289: 24020–29

14. Luo DX, Cao DL, Xiong Y et al: A novel model of cholesterol efflux from lipid-loaded cells. Acta Pharmacol Sin, 2010; 31: 1243–57

15. Wanninger S, Lorenz V, Subhan A, Edelmann FT: Metal complexes of curcumin – synthetic strategies, structures and medicinal applications. Chem Soc Rev, 2015; 44: 4986–5002

16. Chen FY, Zhou J, Guo N et al: Curcumin retunes cholesterol transport homeostasis and inflammation response in M1 macrophage to prevent atherosclerosis. Biochem Biophys Res Commun, 2015; 467: 872–78

17. Bharti AC, Takada Y, Aggarwal BB: Curcumin (diferuloylmethane) inhibits receptor activator of NF-kappa B ligand-induced NF-kappa B activation in osteoclast precursors and suppresses osteoclastogenesis. J Immunol, 2004; 172: 5940–47

18. Zimmermann M: Ethical guidelines for investigations of experimental pain in conscious animals. Pain, 1983; 16: 109–10

19. Zhao YP, Wei JL, Tian QY et al: Progranulin suppresses titanium particle induced inflammatory osteolysis by targeting TNF-alpha signaling. Sci Rep, 2016; 6: 20909

20. Panmekiate S, Ngonphloy N, Charoenkarn T et al: Comparison of mandibular bone microarchitecture between micro-CT and CBCT images. Dentomaxillofac Radiol, 2015; 44: 20140322

21. Huynh NC, Everts V, Nifuji A et al: Histone deacetylase inhibition enhances *in vivo* bone regeneration induced by human periodontal ligament cells. Bone, 2017; 95: 76–84

22. Moss JW, Davies TS, Garaiova I et al: A unique combination of nutritionally active ingredients can prevent several key processes associated with atherosclerosis *in vitro*. PLoS One, 2016; 11: e0151057

23. Kimura T, Nada S, Takegahara N et al: Polarization of m2 macrophages requires lamtor1 that integrates cytokine and amino-acid signals. Nat Commun, 2016; 7: 13130

24. Aggarwal BB, Sung B: Pharmacological basis for the role of curcumin in chronic diseases: An age-old spice with modern targets. Trends Pharmacol Sci, 2009; 30: 85–94

25. Zhao JF, Ching LC, Huang YC et al: Molecular mechanism of curcumin on the suppression of cholesterol accumulation in macrophage foam cells and atherosclerosis. Mol Nutr Food Res, 2012; 56: 691–701

26. Dong SZ, Zhao SP, Wu ZH et al: Curcumin promotes cholesterol efflux from adipocytes related to PPARgamma-LXRalpha-ABCA1 pathway. Mol Cell Biochem, 2011; 358: 281–85

27. Anand P, Kunnumakkara AB, Newman RA, Aggarwal BB: Bioavailability of curcumin: Problems and promises. Mol Pharm, 2007; 4: 807–18

28. Nelson KM, Dahlin JL, Bisson J et al: The essential medicinal chemistry of curcumin. J Med Chem, 2017; 60: 1620–37

29. Gallo J, Goodman SB, Konttinen YT, Raska M: Particle disease: Biologic mechanisms of periprosthetic osteolysis in total hip arthroplasty. Innate Immun, 2013; 19: 213–24